Journal of Modern Optics
Vol. 59, No. 2, 20 January 2012, 166–178

Taylor & Francis
Taylor & Francis Group

Pre-selection of optical transitions in rare-earth ions in crystals perspective for quantum information processing

T.T. Basiev[a], I.T. Basieva[a], A.A. Kornienko[b], V.V. Osiko[a], K.K. Pukhov[a] and S.K. Sekatskii[c]*

[a]*Laser Materials and Technology Center, A.M. Prokhorov General Physics Institute of RAS, Build. 4, Vavilova Str. 38, 119991 Moscow, Russia;* [b]*Vitebsk State Technological University, Moskovsky Prospekt 72, 210035 Vitebsk, Belarus;* [c]*Laboratoire de Physique de la Matière Vivante, IPSB, Ecole Polytechnique Fédérale de Lausanne (EPFL), BSP, CH-1015 Lausanne, Switzerland*

(*Received 18 August 2011; final version received 10 November 2011*)

A systematic analysis of decoherence rates due to electron–phonon interactions for optical transitions of rare-earth dopant ions in crystals is presented in the frame of the point charge model. For this model, the large value of any one of the matrix elements of the unit tensor operator $U^{(k)}$ of rank k for transitions within the 4*f*-electronic configuration, viz. U2, U4 or U6, is enough to ensure the strong optical transition between different levels, while the Stark–Stark transitions within the multiplet can be characterized by the matrix element U2 alone, the influence of elements U4, U6 being of much smaller order of magnitude and neglected. The circumstance that exactly such Stark–Stark transitions within the multiplet define the efficiency of electron–phonon interaction and, consequently, the decoherence rate (except for the case of lowest, less than approximately 2–4 K, temperatures), enables selection of optical transitions which are strong enough and at the same time are characterized by relatively small decoherence rates. Correspondingly, these optical transitions, provided that they lie in an appropriate spectral range and the gap to the nearest neighboring energy level is large enough ($>500\,\mathrm{cm}^{-1}$) to prevent eventual fast phonon-assisted relaxation, should be considered as prospective for subsequent use in quantum informatics processing and communication. The list of such pre-selected transitions is given; the applicability area and limitations of our approach are discussed.

Keywords: spectroscopy; rare-earth ion; crystal; quantum information processing; decoherence

1. Introduction

Optical transitions in rare-earth (RE) dopant ions in crystals have for a long time been used to study coherent optical phenomena. Hence, not surprisingly, they almost from the very appearance of the field of quantum information processing (QIP) and communication started to be considered as a prospective hardware in this field [1]. A number of approaches implying their exploration for these and related topics (such as quantum memory [2] or preparation of light-condensed state quantum interface [3]) has been proposed. We cite, e.g. [4–10], just a few important initial papers, which were followed by numerous subsequent publications.

These proposals are built on different ideas, which, of course, put forward also rather different requirements for optical transitions to be exploited to realize these ideas and achieve the corresponding goals. It is impossible and not relevant for the present paper to discuss all these requirements in detail, but, of course, long decoherence time and convenient spectral range are practically always amongst them. Naturally, this circumstance has been recognized, and in the literature a number of papers discussing aspects of the problem can be found (see [2,11–13] and especially recent books [14,15]). However, it should be noted that almost exclusively only optical transitions originating from the ground state of a RE ion have been analyzed, and it appears that not even all of them were indeed studied. Strange as it may seem, our search shows that the systematic analysis of numerous optical transitions in rare-earth dopant ions aiming their 'pre-selection' exactly from this point of view, i.e. which transitions, lying in a practically accessible spectral range and sufficiently intense, at the same time at certain conditions are characterized by large decoherence (dephasing) time, is apparently still lacking in the literature.

In this note we would like to start such an analysis. We limit ourselves to the spectral line broadening caused by electron–phonon interactions. Thus our analysis is not applicable for the lowest temperatures,

*Corresponding author. Email: serguei.sekatski@epfl.ch

ISSN 0950–0340 print/ISSN 1362–3044 online

http://dx.doi.org/10.1080/09500340.2011.640949
http://www.tandfonline.com

smaller than approximately 2–4 K for the most crystals and rare earth ions, where not electron–phonon broadening but other factors (such as ion–ion or magnetic interactions) are usually of the uttermost importance, and it is not relevant for irregular media and glasses where low-frequency tunneling processes caused by so-called two-level systems (TLS) are very important. Also our picture, where electron–phonon interaction is considered in the frame of the point charge model, which is not always able to catch all important parameters of concrete optical transitions in real crystals, is evidently a rather simple one, and we insist that this is really a pre-selection only; a detailed theoretical and experimental study of any optical transition aspiring to be suitable for QIP is actually needed.

Still, we hope that the proposed approach will be useful for specialists in the field. First, this is because the model presented, and this is a good side of its simplicity, is general enough and quite transparent so our conclusions and findings are clear and easy to implement, while the results can be verified by experimental data. Second, our simple model nevertheless goes beyond the usually applicable, and inappropriate for the quantum informatics field, 'zero-order' approximation based only on the gap in the Stark level picture of rare-earth ions in crystals, ignoring all other important characteristics of these ions.

As an exception of this oversimplified energetic gap law approach we can indicate papers [16,17] where symmetric non-monotonic changes of the ion–ligand electromagnetic interaction intensity (spectral broadening and vibronic transition strength) for the family of lanthanide ions were presented. Discovering the decrease of electron–phonon interaction along the RE row, the authors, however, did not go on to address the characteristics of the electron levels and optical transitions.

Yet the electron–phonon interaction strength does not just change along the rare-earth row but directly depends on the type of electron levels involved in the transition, as we pioneered in demonstrating in [18] for multiphonon non-radiative relaxation of RE ions in crystals. These observations led us to develop the present model, where we tried to consistently trace back the connection between the rates of direct one-phonon relaxation transitions within Stark sublevels of a multiplet and the electron matrix elements, U2, U4 and U6, which characterize the term's electron properties. In so doing, we put aside the type of the crystal lattice and the value of Stark splitting. On the basis of the model, we suggest an algorithm for finding the most perspective ions and transitions of minimal dephasing, relatively long quantum states lifetime, and optical transitions dipole or quadrupole moments large enough to expect strong coherent interaction of RE ions with each other and with resonant laser radiation. The next step should be the choice of a suitable crystal matrix in which the induced optical electro-dipole intermultiplet transitions of RE dopants could be amplified, while the relaxation of one- and multiphonon, decohering, transitions would be weakened.

2. Theoretical framework

The general theory of the broadening of electronic transitions in rare-earth ions in solids caused by an electron–phonon interaction is nowadays rather well established and a good exposition can be found, for example, in [14–17,19–24]. For this reason, in this section we give only a very short presentation of the theoretical framework, limiting it to the minimum necessary for our subsequent analysis.

The density matrix formalism gives the most consistent description of relaxation processes [25–27]. The equation for density matrix σ of a quantum dynamical subsystem with discrete states (atom, ions, molecules, quantum dots, electron or nuclear spins, etc.), which interacts with a dissipative medium (thermal bath), can be written as [27]:

$$\dot{\sigma}(t) = -\frac{i}{\hbar}[H_0, \sigma(t)] - \frac{1}{\hbar^2}\int_0^\infty Sp_f[V(0), [V(-\tau), \rho_T\sigma(t)]]\mathrm{d}\tau. \tag{1}$$

Hereafter we will refer to this subsystem as an electronic subsystem, and to its interaction with the thermostat as an electron–phonon interaction (EPI), aiming at future application of the theory to rare-earth ions in a crystal. In Equation (1), H_0 is the Hamiltonian of a RE ion in a static crystal field (CF),

$$\rho_T = \exp(-H_L/kT)/Sp_f \exp(-H_L/kT) \tag{2}$$

is the thermal-equilibrium density matrix of the lattice (thermal bath) Hamiltonian H_L and temperature T, subscript f in Sp_f indicates a summation over thermal bath variables f and

$$V(t) = \exp\{i(H_0 + H_L)t/\hbar\}\ V \exp\{-i(H_0 + H_L)t/\hbar\}. \tag{3}$$

In Equation (3) the Hamiltonian of EPI V is defined as:

$$V = H' - \langle H' \rangle, \tag{4}$$

where H' is the Hamiltonian of the interaction of dynamic and dissipative subsystems (hereafter angle brackets denote the averaging over the thermostat: $\langle A \rangle = Sp_f \rho_T A$), thus $\langle V \rangle = 0$. The thermal mean value

$\langle H' \rangle$ enters H_0 and is responsible for the temperature shift of electronic levels.

It should be noted that Equation (1) is valid for the case when one can neglect the transformation of the Hamiltonian H_L due to the electron transitions. The Huang–Rhys–Pekar parameter S of electron–phonon coupling is the quantitative measure of this transformation [21]. RE ions belong to the systems with extremely weak electron–phonon coupling, $S \ll 1$. For example, the calculations of Malkin [24] give $S = 0.0028$ for Er^{3+} (transition $^4F_{5/2}$–$^4F_{7/2}$) and $S = 2.6$–4.3×10^{-4} for Nd^{3+} (transition $^2H_{11/2}$–$^4G_{5/2}$) in a $LiYF_4$ crystal. For comparison, in F-centers, for which such parameters have been first defined, parameter $S \sim 10$.

If the width of the electron transition $g \Leftrightarrow g'$ is much smaller than the transition frequency $\omega_{gg'}$, Equation (1) gives the balance equations:

$$\dot{\sigma}_{gg} = -\sum_{g'} W_{gg'}\sigma_{gg} + \sum_{g'} W_{g'g}\sigma_{g'g'} \tag{5}$$

for diagonal elements of the density matrix (level populations), and

$$\dot{\sigma}_{gg'} = -i(\omega_{gg'} + \Delta\omega_{gg'})\sigma_{gg'} - \gamma_{gg'}\sigma_{gg'}, \quad (g \neq g') \tag{6}$$

for non-diagonal elements of the density matrix. The value $\Delta\omega_{gg'}$ here is the relaxation shift of the line.

In balance Equations (5), σ_{gg} is the population of the gth state of the electron subsystem, $W_{gg'}$ is the probability of the relaxation transition $g \to g'$ induced by interaction V. In Equations (6) for the non-diagonal elements of the density matrix

$$\gamma_{gg'} = \gamma_{gg'}^{(rel)} + \gamma_{gg'}^{(ad)}, \tag{7}$$

where

$$\gamma_{gg'}^{(rel)} = \frac{1}{2}\sum_{g''}(W_{gg''} + W_{g'g''}), \tag{8}$$

is a contribution to the relaxation transition line width (relaxation broadening), and

$$\gamma_{gg'}^{(ad)} = \int_{-\infty}^{\infty} \left\langle \left[V_{gg}(\tau) - V_{g'g'}(\tau)\right]\left[V_{gg} - V_{g'g'}\right]\right\rangle \mathrm{d}\tau \tag{9}$$

is the so-called adiabatic broadening (or pure dephasing).

The value $\gamma_{gg'} = 1/T_{gg'}$ is equal to the rate of dephasing of a non-diagonal element of the density matrix:

$$\sigma_{gg'}(t) = \exp[-i(\omega_{gg'} + \Delta\omega_{gg'})t - t/T_{gg'}]\sigma_{gg'}(0). \tag{10}$$

Specifically, $T_{gg'}$ is the time of the free-induction decay for homogeneous lines.

According to Equation (6), the normalized zero-phonon line (ZPL) of the transition $g \Leftrightarrow g'$ has the Lorentzian form:

$$G_{gg'}(\Omega) = \frac{1}{\pi}\frac{\gamma_{gg'}}{(\omega_{gg'} + \Delta\omega_{gg'} - \Omega)^2 + (\gamma_{gg'})^2} \tag{11}$$

with the homogeneous full width at half maximum (FWHM) equal to $2\gamma_{gg'}$.

2.1. Adiabatic phonon-induced broadening

As can be seen from Equation (9), adiabatic broadening $\gamma_{gg'}^{(ad)}$ is defined by the spectral density at zero frequency dependent on the correlator $\langle[V_{gg}(\tau) - V_{g'g'}(\tau)] \times [V_{gg} - V_{g'g'}]\rangle$, which, in turn, depends on the difference between the diagonal elements of the matrix of electronic perturbations V.

Let us introduce Taylor expansion of the interaction potential V:

$$\begin{aligned} V &= \sum V_{S\alpha}^{(1)} u_\alpha^{(S)} + V_{S\alpha,S'\alpha'}^{(2)}\left[u_\alpha^{(S)}u_{\alpha'}^{(S')} - \langle u_\alpha^{(S)}u_{\alpha'}^{(S')}\rangle\right] + \cdots \\ &= \sum \frac{\partial V}{\partial u_\alpha^{(S)}} u_\alpha^{(S)} + \frac{1}{2}\frac{\partial^2 V}{\partial u_\alpha^{(S)}\partial u_{\alpha'}^{(S')}}\left[u_\alpha^{(S)}u_{\alpha'}^{(S')} - \langle u_\alpha^{(S)}u_{\alpha'}^{(S')}\rangle\right] + \cdots \end{aligned} \tag{12}$$

where $u_\alpha^{(S)}$ is the αth component of the displacement vector $\mathbf{u}_S = \mathbf{u}_S(L) - \mathbf{u}(RE)$, $\mathbf{u}(RE)$ and $\mathbf{u}_S(L)$ are the displacements of the RE ion and the Sth ligand from their equilibrium positions; the summing is over the (nearest) ligands and displacement vector components. In the harmonic approximation of lattice vibrations, linear with respect to a small displacement of lattice ions from their equilibrium positions terms $V^{(1)}u$ affect $\gamma_{gg'}^{(ad)}$ only in the second order of the perturbation theory [23]. In the Debye model of lattice vibrations, contribution to $\gamma_{gg'}^{(ad)}$ from quadratic terms $V^{(2)}u^2$ leads to the temperature dependence given by McCumber and Sturge formula [19]:

$$\gamma_{gg'}^{(ad)} = C_{gg'}\left(\frac{T}{\theta}\right)^7 \int_0^{\theta/T} x^6 \exp(x)[\exp(x) - 1]^{-2}\,\mathrm{d}x, \tag{13}$$

where θ is the Debye temperature. This contribution acts together with the direct relaxation processes (see the next section) and dominates when there is no Stark splitting of the levels in the crystal field.

2.2. Relaxation phonon-induced broadening

The relaxation broadening depends on non-diagonal matrix elements of the perturbation V. For trivalent rare-earth ions having a branched Stark-level structure which spectrum is dipped into the phonon spectrum of crystalline host, the predominant contribution to the

relaxation probabilities $W_{gg'}$ is given, in general, by one-phonon (direct) transitions between Stark levels. So, the main contribution to relaxation broadening $\gamma_{gg'}^{(rel)}$ comes from direct transitions between Stark components within multiplets J and J', i.e. from interaction terms $V^{(1)}u$. (The exceptions are closely-spaced J- and J'-multiplets and the cases with $J+J'<2$; see selection rules below.) Thus, we can write for optical transitions $Ji \Leftrightarrow J'j$:

$$\gamma^{(rel)}(Ji, J'j) = \frac{1}{2}\sum_{i'} W(Ji \to Ji') + \frac{1}{2}\sum_{j'} W(J'j \to J'j') \tag{14}$$

with

$$W(Ji \to Ji') = \frac{1}{\hbar^2}\sum_{\alpha\beta SS'} \left(Ji|V_{S\alpha}^{(1)}|Ji'\right)\left(Ji'|V_{S'\beta}^{(1)}|Ji\right) \times \int_{-\infty}^{\infty} \exp(i\omega_{ii'})\langle u_{S\alpha}(\tau)u_{S'\beta}\rangle \mathrm{d}\tau. \tag{15}$$

Subscripts i, i' (j,j') here identify the Stark components of the J-multiplet (J'-multiplet):

$$|Ji) = \sum_M C_M^{(i)}|JM), \tag{16}$$

and $\hbar\omega_{ii'} = E_{Ji} - E_{Ji'} \equiv \Delta_{ii'}$ is the energy difference of Stark components.

In the framework of the crystal field model of the electron–lattice interaction the term $V_{S\alpha}^{(1)}$ can be written as

$$V_{S\alpha}^{(1)} = \sum_{km} B_{kmS\alpha}^{(1)} \sum_a Y_{km}(\xi_a), \tag{17}$$

where Y_{km} is a spherical harmonic and $\boldsymbol{\xi}_a$ is an instantaneous radius vector of the a-th $4f$-electron with respect to the nucleus of the rare-earth ion. Therefore, the matrix elements $\langle Ji|V_{S\alpha}^{(1)}|Ji'\rangle$ can be represented as:

$$\left(Ji|V_{S\alpha}^{(1)}|Ji'\right) = \sum_{km} B_{kmS\alpha}^{(1)} \sum C_M^{(i)*} C_{M'}^{(i')} \left(JM|\sum_a Y_{km}(\xi_a)|JM'\right). \tag{18}$$

According to the Wigner–Eckart theorem [28]

$$\left(\gamma JM\left|\sum_a Y_{km}(\xi_a)\right|\gamma' J'M'\right) = (-1)^{J-M}\begin{pmatrix} J & k & J' \\ -M & m & M' \end{pmatrix}(l\,||\,Y_k||l)\left(\gamma J||U^{(k)}||\gamma' J'\right), \tag{19}$$

where

$$(l\|\,Y_k\|l) = (-1)^l\begin{pmatrix} l & k & l \\ 0 & 0 & 0 \end{pmatrix}\left[\frac{(2l+1)(2k+1)(2l+1)}{4\pi}\right]^{1/2}, \tag{20}$$

and γ are the quantum numbers not associated with the angular momentum $\boldsymbol{J}$.

In Equations (19) and (20), l is the orbital angular momentum of the optical electron ($l=3$ for the $4f$-electron); $\left(\begin{smallmatrix} J & k & J' \\ -M & m & M' \end{smallmatrix}\right)$ is the 3j-symbol; and $\left(\gamma J\|\,U^{(k)}\|\,\gamma J\right)$ is the diagonal reduced matrix element of the unit tensor operator $U^{(k)}$ of rank k for the transitions within the $4f$-electronic configuration.

2.3. Radiative intermultiplet transitions

According to Judd–Ofelt theory [29,30], the rate of radiative electro-dipole inter-multiplet $J \to J'$ transition is proportional to the line strength

$$S(J,J') = \Omega_2\left(\gamma J\|\,U^{(2)}\|\,\gamma' J'\right)^2 + \Omega_4\left(\gamma J\|\,U^{(4)}\|\,\gamma' J'\right)^2 + \Omega_6\left(\gamma J\|\,U^{(6)}\|\,\gamma' J'\right)^2.$$

2.4. Selection rules for $U^{(k)}$

Matrix elements $\left(\alpha SLJ\|\,U^{(k)}\|\,\alpha' S'L'J'\right)$ do not vanish if the 'triangle rule' holds:

$$\left|J - J'\right| \le k \le J + J'. \tag{21}$$

Hence, the diagonal elements

$$\left(J\|\,U^{(k)}\|\,J\right) = 0 \quad \text{if } k > 2J. \tag{22}$$

The condition

$$S = S' \tag{23}$$

and the triangle rule

$$\left|L - L'\right| \le k \le L + L' \tag{24}$$

are not strict selection rules. However, it is often that $\left|\left(SLJ\|\,U^{(k)}\|\,S'L'J'\right)\right| \ll 1$ when the conditions of Equations (23)–(24) do not hold.

3. Perspective optical transitions in rare-earth ions

It follows from Equations (18)–(20) that the matrix element $(Ji|V_{S\alpha}^{(1)}|Ji')$ for a three-valent rare-earth ion is of the form

$$\left(Ji|V_{S\alpha}^{(1)}|Ji'\right) = {\sum_k}' A_{kS\alpha}^{(1)}(i,i')\left(\gamma J\|\,U^{(k)}\|\,.\gamma J\right), \tag{25}$$

with $k = 2, 4, 6$. Correspondingly, the relaxation broadening $\gamma^{(rel)}(Ji, J'j)$ of the $g \Leftrightarrow g'$ transition is mainly

determined by the squares of the diagonal reduced matrix elements $(\gamma J\|U^{(k)}\|\gamma J)$ and $(\gamma' J'\|U^{(k)}\|\gamma' J')$. Below we limit ourselves with the point charge model where ligands are considered as localized point charges with an effective q value. In such a model the factors $A^{(1)}_{kS\alpha}(i,i')$ are proportional to $(\overline{\xi^k}/R^k)$ where $\overline{\xi^k}$ is the mean value of the kth power of the $4f$-electron radius ξ and R is the equilibrium rare earth ion–ligand distance. Correspondingly, the relative contributions of the squares of $(\gamma J\|U^{(k)}\|\gamma J)$ and $(\gamma' J'\|U^{(k)}\|\gamma' J')$ matrix elements are proportional to $(\overline{\xi^k}/R^k)^2$. Due to the inequality $(\overline{\xi^2}/R^2)^2 \gg (\overline{\xi^4}/R^4)^2 \gg (\overline{\xi^6}/R^6)^2$ which evidently holds true for the rare-earth ions in solids, in the frame of our model we can neglect the broadening caused by terms depending on the diagonal reduced matrix elements $(\gamma J\|U^{(k)}\|\gamma J)$ and $(\gamma' J'\|U^{(k)}\|\gamma' J')$ with the value of k greater than $k=2$, so we have that in our model the relaxation broadening is determined only by the squares of the expressions $(\gamma J\|U^{(2)}\|\gamma J)$ and $(\gamma' J'\|U^{(2)}\|\gamma' J')$.

Analogous analysis shows that this same conclusion remains valid also for the adiabatic broadening where, as we have stated above, the contributions to $\gamma^{(ad)}_{gg'}$ come either from quadratic $V^{(2)}u^2$ terms or, in the second order of the perturbation theory, from linear $V^{(1)}u$ terms [23]. Relative contributions of these terms are proportional respectively to $(\overline{\xi^k}/R^k)^2$ or $(\overline{\xi^k}/R^k)^4$ hence similarly the terms dependent on the diagonal reduced matrix elements $(\gamma J\|U^{(k)}\|\gamma J)$ and $(\gamma' J'\|U^{(k)}\|\gamma' J')$ with the value of $k=2$ contribute most.

All this means that, under otherwise equal conditions, the rate of the one-phonon relaxation transition will be the greater, the greater the value of $(J\|U^{(2)}\|J)^2$ is and, correspondingly, for a given *RE* ion the broadening of the optical transition $J \Leftrightarrow J'$ will be the smaller, the smaller the matrix elements $(J\|U^{(k)}\|J)$ and $(J'\|U^{(k)}\|J')$ are, all other factors being the same. Analysis of optical transitions $J \Leftrightarrow J'$ from this point of view will be given in the next section.

3.1. *Pre-selection of perspective optical transitions for real rare-earth ions*

Direct connection between the dephasing in RE ions (or Stark–Stark transition spectral line broadening) and individual properties of their electron transitions, which was established above, makes possible a preliminary selection of the most perspective transitions for performing quantum informatics experiments: using the known values of the squares of matrix elements $(\gamma J||U^{(k)}||\gamma J)^2$ with $k=2$, 4, 6 (below we will refer to these values simply as, respectively, U2, U4 and U6) we have selected strong enough and having relatively small decoherence electronic transitions. We took into account the transitions with an energy not essentially greater than 30,000 cm^{-1}, i.e. the spectral range where most existing lasers operate. Besides, we did not consider transitions to/from levels having the next lower level closer than 500 cm^{-1} (to which fast relaxation may occur). The values of U2, U4 and U6 for gadolinium and thulium ions were taken from the tables given by Carnall et al. [31]; for all other rare-earth ions the squares of corresponding matrix elements have been calculated anew following the procedure presented in [32,33] (a part of the values pertinent for erbium and neodymium ions actually can be found in these earlier papers) and using the parameters of the Hamiltonian (quasi-free ion approximation) given in [34,35]. Details of these calculations will be published elsewhere.

To summarize again: in the frame of our model the high value of any one (or few) matrix elements U2, U4 and U6 is enough to ensure the strong optical transition between inter-multiplet levels while the Stark–Stark transition within one multiplet can be characterized by the matrix element U2 alone, because the influence of elements U4 and U6 is of higher order and can be neglected. Of course, 'strong optical transition' is a relative term, so in practice we were obliged to limit ourselves to certain concrete values of matrix elements at question to judge whether a transition is strong or not. All relevant values are given in our tables and figures below. Roughly, we may say that the transitions with the values of U2, U4 and U6 (or their sum) exceeding approximately 0.15 were considered as strong enough for all rare-earth elements except some of samarium. This is justified by the circumstance that the decoherence-related inter-level U2 values for samarium are also considerably (at least

Table 1. Parameters of perspective optical transitions in Tm^{3+} and Gd^{3+}.

Ion	Initial level	Gap to the next lower level (cm^{-1})	U2 of intralevel transitions	Final level	Gap to the next lower level (cm^{-1})	U2 of intralevel transitions	Energy of the transition (cm^{-1})	Transition matrix elements U2, U4, U6
Gd^{3+}	$^6P_{5/2}$	595	0.03	$^6I_{7/2}$	2551	0.005	3122	U6 = 0.707
Tm^{3+}	$^3F_4$	5610	0.01	$^3P_0$	750	0	29,824	U4 = 0.27

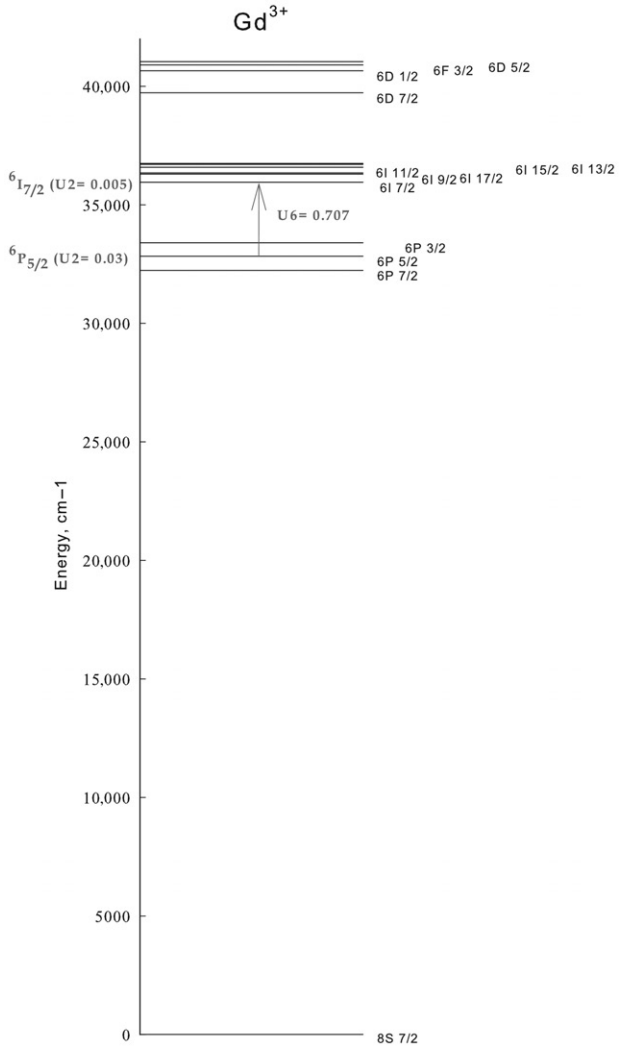

Figure 1. Perspective optical transitions in Gd^{3+}: $^6P_{5/2} \rightarrow {}^6I_{7/2}$.

five times) smaller than their homologues for other rare-earth ions.

Following this procedure, we have found only one appropriate transition for Gd^{3+} and one for Tm^{3+} ions (see Table 1 and Figures 1 and 2). For Gd^{3+} ions, it is an optical transition in the middle infrared, between $^6P_{5/2}$ and $^6I_{7/2}$ levels. It has a high value of matrix element $U6 = 0.707$, which allows us to expect a considerable value of the optical transition dipole moment in non-centrosymmetrical crystals. Meanwhile, the matrix elements of Stark–Stark transitions of the initial and final states are very small: U2 ($^6P_{5/2}$–$^6P_{5/2}$) = 0.03 and U2 ($^6I_{7/2}$–$^6I_{7/2}$) = 0.004. At the same time, the energy gaps to the next lower levels are fairly large (595 and 2551 cm^{-1}), limiting the rate of the multiphonon downrelaxation in crystals with a short phonon spectrum. A similar situation occurs for Tm^{3+}

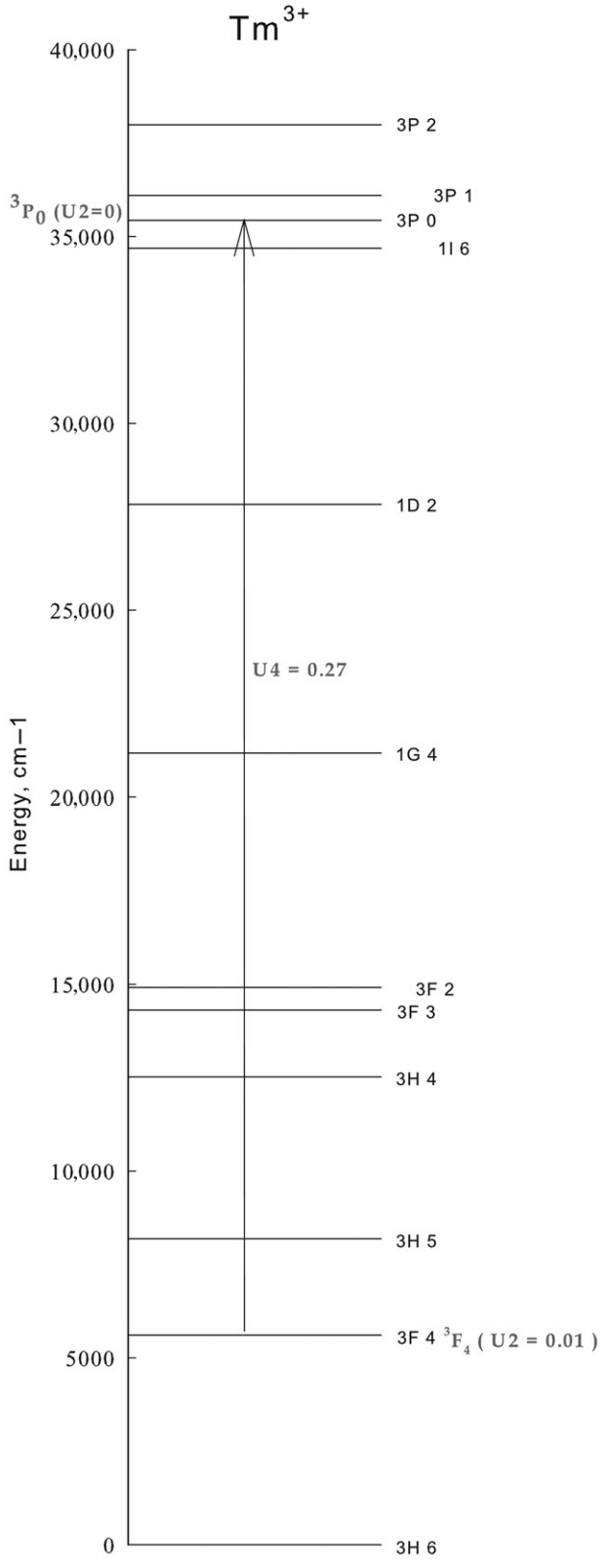

Figure 2. Perspective optical transitions in Tm^{3+}: $^3F_4 \rightarrow {}^3P_0$.

Table 2. Parameters of perspective optical transitions in Pr^{3+} and Sm^{3+}.

Ion	Initial level	Gap to the next lower level (cm^{-1})	U2 of intralevel transitions	Final level	Gap to the next lower level (cm^{-1})	U2 of intralevel transitions	Energy of the transition (cm^{-1})	Transition matrix elements U2, U4, U6
Pr^{3+}	$^3F_2$	653	0.0618	$^3P_0$	3866	0.00	15,557	U2 = 0.2954
	$^3F_3$	1391	0.0625	$^3P_1$	624	0.01607	14,790	U2 = 0.5714 U4 = 0.1964
	$^3F_4$	433	0.0135	$^1G_4$	2912	0.0004	2912	U2 = 0.0796 U4 = 0.1471 U6 = 0.3574
Sm^{3+}	$^6F_{5/2}$	492	0.001	$^4P2_{5/2}$	1188	0.006	25,598	U2 = 0.023 U4 = 0.049
	$^6F_{7/2}$	848	0.003				24,750	U2 = 0.014 U4 = 0.028
	$^4F3_{3/2}$	964	0.002	$^4P2_{1/2}$	918	0.006	12,259	U2 = 0.058
	$^4H1_{7/2}$	698	0.009	$^4I2_{9/2}$	467	0.002	9074	U2 = 0.047 U4 = 0.061 U6 = 0.061

ions with the difference that the optical transition lays in the ultraviolet range $h\upsilon = 29{,}824\,cm^{-1}$, connecting the $^3F_4$ and $^3P_0$ levels. The matrix element of this optical transition (defining the transition strength and dipole moment value) is also quite big (U4 = 0.27), and Stark–Stark are still weaker: U2 ($^3F_4$–$^3F_4$) = 0.01; U2 ($^3P_0$–$^3P_0$) = 0. Gaps to lower levels are also large: 5610 and 750 cm^{-1}.

The situation is somewhat more diverse for Pr^{3+} and Sm^{3+} ions (see Table 2 and Figures 3 and 4). Here the transitions from the ground state are not presented, due to the fact that the matrix elements U2 ($^3H_4$–$^3H_4$) = 0.7788 and U2 ($^6H_{5/2}$–$^6H_{5/2}$) = 0.3879 are big and account for the fast decoherence of the ground state. In some cases, wider spectra can be of interest for practical use in laser materials and luminophores (for example, a large broadening value is useful for broadband and tunable lasing), but in the case of quantum experiments decoherence is the main limitation. For Pr^{3+} ions, the optical transition $^3F_4 \rightarrow {}^1G_4$ ($h\upsilon = 5912\,cm^{-1}$, U4 = 0.14; U6 = 0.357) could be of interest due to a smaller than expected decoherence and spectral line broadening, which is because U2 ($^3F_4$–$^3F_4$) = 0.0135 and U2 ($^1G_4$–$^1G_4$) = 0.0004. Also, we chose the optical transition $^3F_2 \rightarrow {}^3P_0$ (U2 = 0.2954; $h\upsilon = 15{,}557\,cm^{-1}$) with U2 ($^3F_2$–$^3F_2$) = 0.06 and U2 ($^3P_0$–$^3P_0$) = 0, and a somewhat stronger optical transition $^3F_3 \rightarrow {}^3P_1$ (U2 = 0.57; U4 = 0.1964; $h\upsilon = 14{,}790\,cm^{-1}$), which, however, also has a faster dephasing: U2 ($^3F_3$–$^3F_3$) = 0.0625, U2 ($^3P_1$–$^3P_1$) = 0.16. While for Sm^{3+} we can find a number of slowly relaxing levels with the weak expectable decoherence U2 = 0.002–0.006, the optical transitions themselves are also weak (U2 = 0.01–0.06).

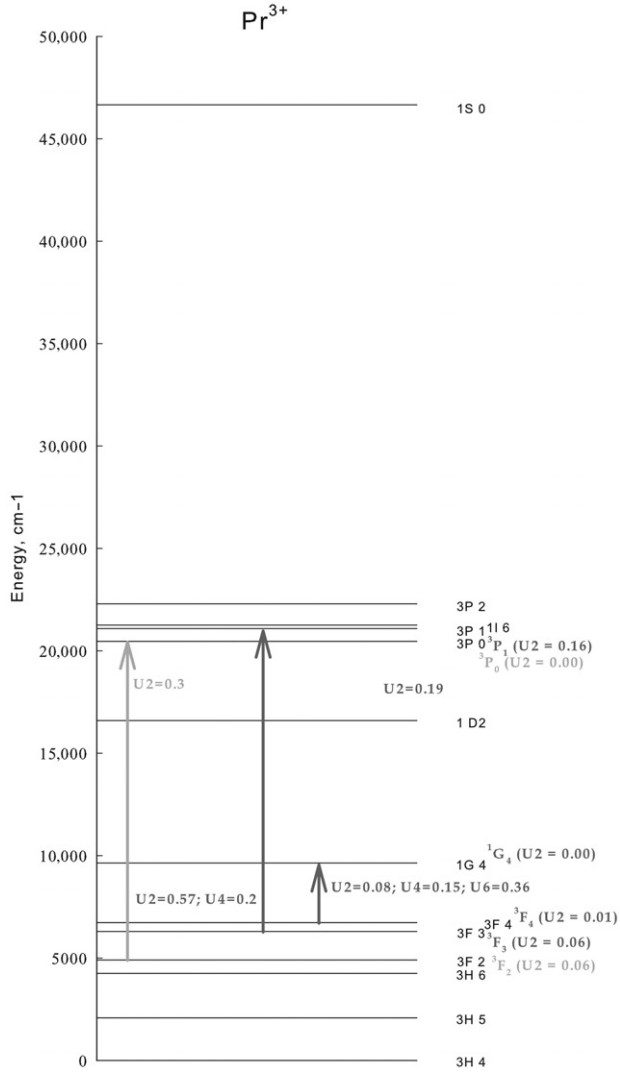

Figure 3. Perspective optical transitions in Pr^{3+}.

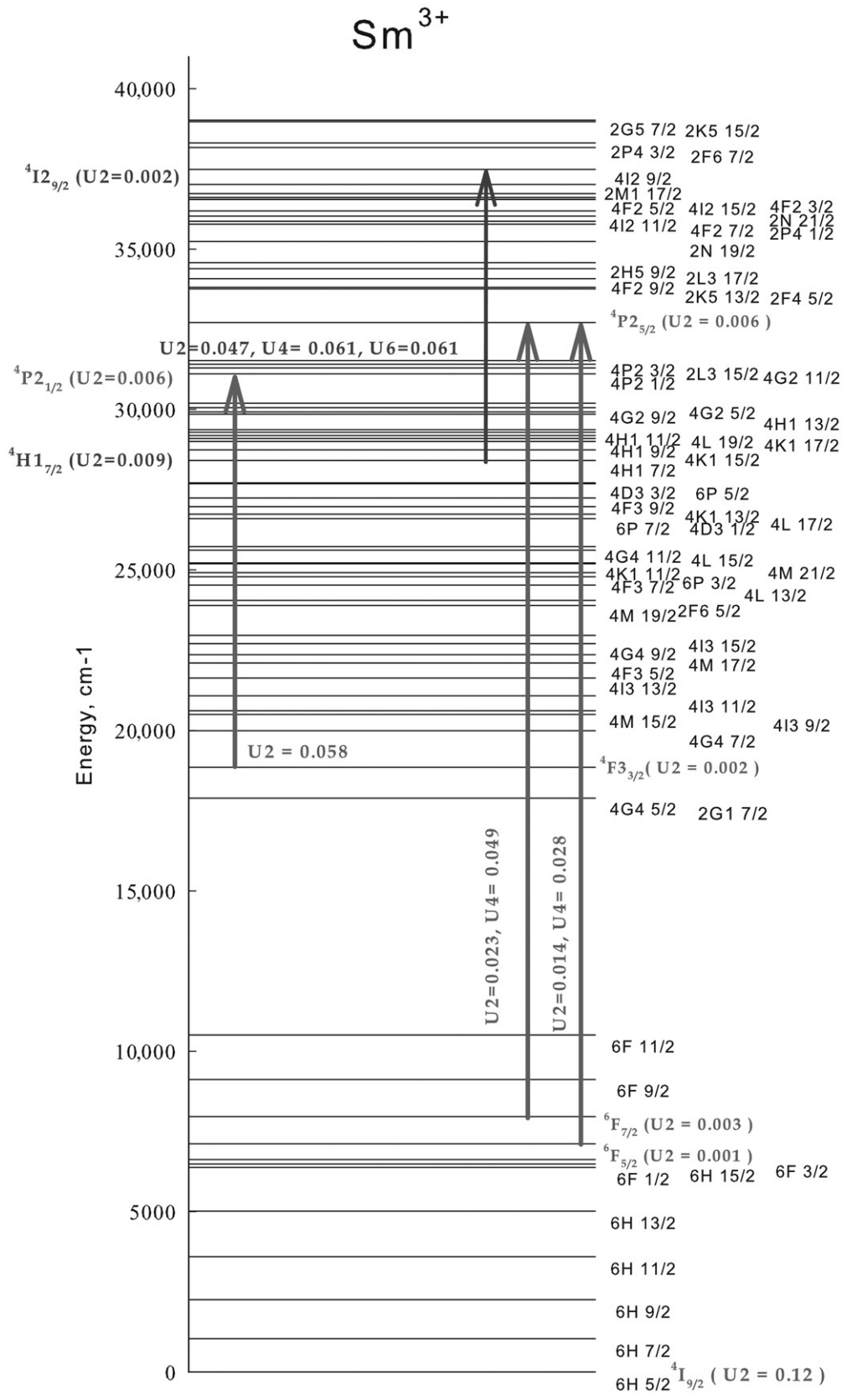

Figure 4. Perspective optical transitions in Sm^{3+}.

Table 3. Parameters of perspective optical transitions in Nd^{3+}.

Ion	Initial level	Gap to the next lower level (cm^{-1})	U2 of intralevel transitions	Final level	Gap to the next lower level (cm^{-1})	U2 of intralevel transitions	Energy of the transition (cm^{-1})	Transition matrix elements U2, U4, U6
Nd^{3+}	$^2P_{1/2}$	1576	0	$^2F2_{7/2}$	1422	0.05	16,787	U4 = 0.17
	$^2H2_{11/2}$	1189	0.011				23,883	U2 = 0.95
								U4 = 1
	$^4G_{5/2}$	1123	0.003	$^4D_{3/2}$	2053	0.007	11,146	U2 = 0.179
	$^4S_{3/2}$	721	0.0006				14,853	U2 = 0.23
	$^4S_{3/2}$	721	0.0006	$^4G_{5/2}$	1123	0.003	3707	U2 = 0.177
	$^4F_{5/2}$	1047	0.044				4593	U2 = 0.268
								U4 = 0.129
	$^4F_{3/2}$	5446	0.062				5640	U2 = 0.483
								U4 = 0.044
	$^4I_{9/2}$	0	0.12				17,036	U2 = 0.8979
								U4 = 0.409
								U6 = 0.036

For Nd^{3+} ions, the matrix element U2 = 0.8979 predicts a strong optical transition from the ground level $^4I_{9/2}$ (U2 = 0.12) to the $^4G_{5/2}$ level (U2 = 0.003, the gap to the nearest lower level is 1123 cm^{-1}) with the transition energy $h\upsilon = 17{,}036\,cm^{-1}$. Besides, in Nd^{3+}, the very strong transition from the $^2H2_{11/2}$ level (U2 = 0.011) to the $^2F2_{7/2}$ (U2 = 0.05) level is suggested, due to the elements U2 = 0.95 and U4 = 1.00. Among the transitions with smaller energies, we point out the strong transition (U2 = 0.483, U4 = 0.044, $h\upsilon = 5640\,cm^{-1}$) from the $^4F_{3/2}$ level (U2 = 0.062) to the same $^4G_{5/2}$ level. Besides, some more transitions that satisfy our conditions have been found in Nd^{3+} (see Table 3 and Figure 5).

The situation when transitions from a few different levels to the same one with the small decoherence seem effective repeats for the following rare-earth ions: Er^{3+}, Dy^{3+} and Eu^{3+} (see Figures 6–8, respectively). For example, for Er^{3+} ions, three transitions to the $^4D_{5/2}$ level (U2 = 0.001) are found: from $^4S_{3/2}$ (U2 = 0.037), $^4F_{5/2}$ (U2 = 0.015), $^4G_{9/2}$ (U2 = 0.001) levels. The matrix elements of these transitions are about 0.2, and the gaps to the nearest lower levels (3217 cm^{-1}, 1652 cm^{-1} and 978 cm^{-1}) promise reasonable probabilities of multiphonon relaxation (Table 4).

In Dy^{3+} ions, very dense disposition of levels makes the selection by the gap to the next lower level essential. Two pairs of transitions – to $^2H1_{9/2}$ (U2 = 0.00) and $^6P_{3/2}$ (U2 = 0.04) – satisfy our demands. Details on the transitions are shown in Table 5 and Figure 7. Let us note that, along with relatively small interlevel gaps, the matrix elements of inter-Stark transitions U2 are close to zero and are minimal among the selected transitions in all ions of the series, which promises adequate dephasing times.

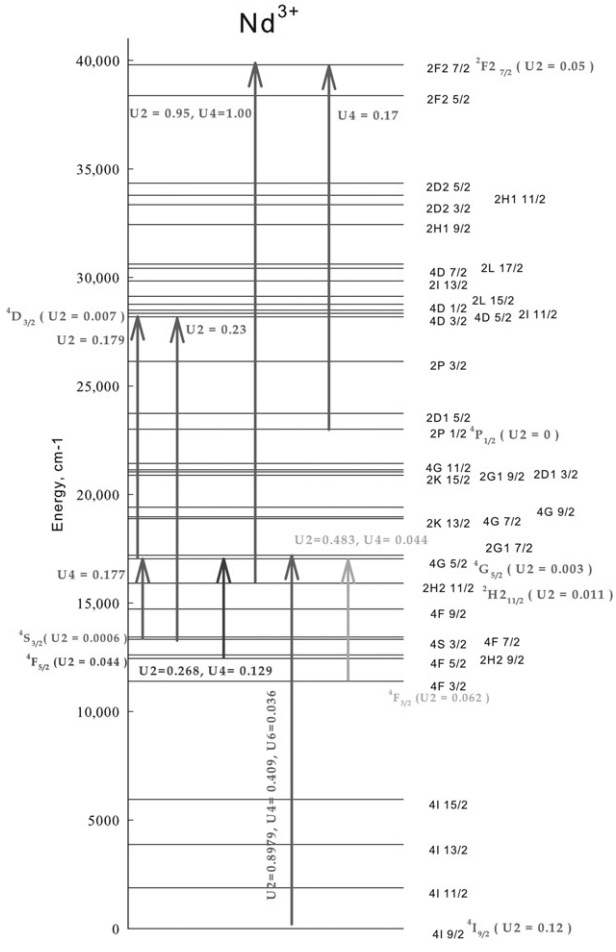

Figure 5. Perspective optical transitions in Nd^{3+}.

Three transitions satisfying our conditions have been chosen in Eu^{3+}: two from $^5D_2$ level and one from

$^5D_0$ level (U2 = 0.003), which is spaced from all lower-energy levels by at least 12,000 cm^{-1} (see Table 6 and Figure 8). Note, that electric-dipole transitions $^7F_0 \leftrightarrow {}^5D_{Jodd}$, $^7F_{Jodd} \leftrightarrow {}^5D_0$ and $^7F_0 \leftrightarrow {}^5D_0$ in Eu^{3+} are forbidden within the standard Judd–Ofelt theory (see [36–38] and references therein), and for this reason we did not consider the transitions involving the ground state multiplet $^7F_0$ of the europium ion.

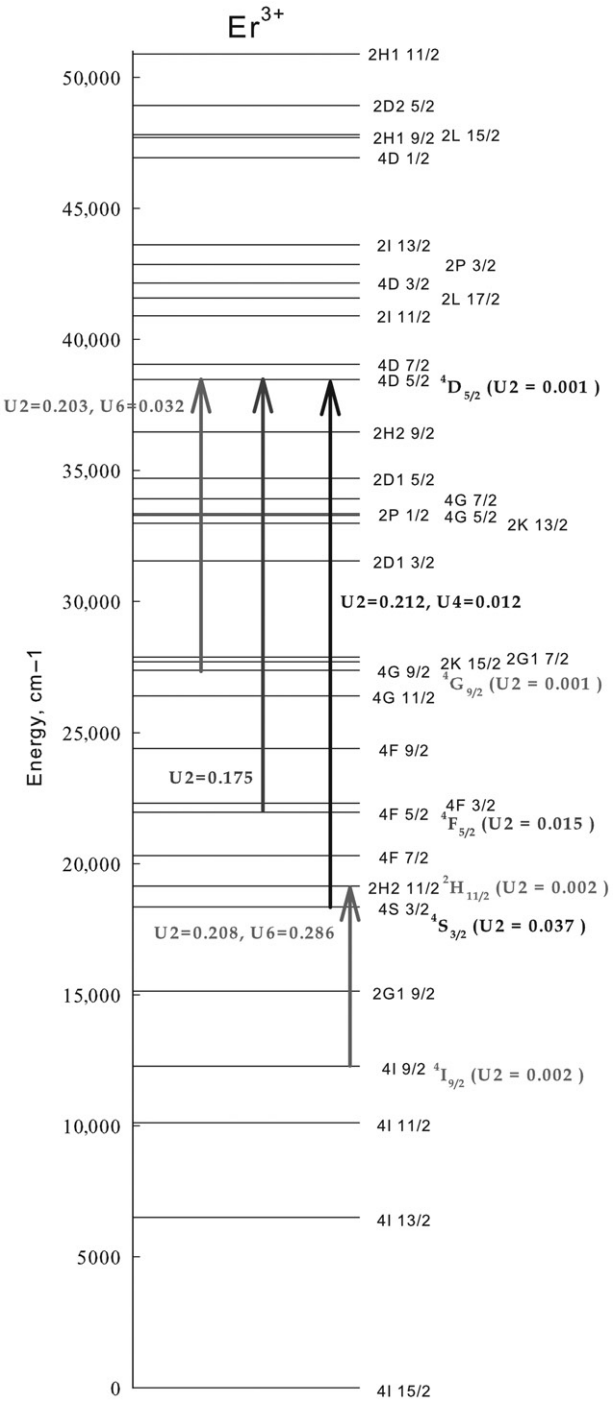

Figure 6. Perspective optical transitions in Er^{3+}.

4. Conclusion

Strong optical transitions with relatively small decoherence rates in rare-earth ions have been selected based on matrix elements U2, U4 and U6. Theoretical justification of the selection procedure, together with its applicability area and limitations, are presented. As a result, we propose a sufficiently large number of optical transitions in rare-earth ions which look quite suitable for QIP experiments.

What, however, came as some surprise, at least for the authors of the present paper, is the fact that transitions involving the ground state of ions are *not* present in our list apart from only one transition, viz. the $^4I_{9/2}$–$^4G_{5/2}$ transition of Nd^{3+}, a transition which has been used by us for first QIP experiments based on resonant interactions between RE ions [39], and where quite large decoherence T_2 times equal to 6.3 ns for a temperature of 9 K and to 1.2 ns for the temperature of 18 K have been experimentally measured in CaF_2 crystals even for a pair of neodymium M-centers [40]. It turns out that for all such transitions, including those which are actually used or considered to be used in QIP-type experiments, such as $^3H_4 \rightarrow {}^1D_2$ in Pr,

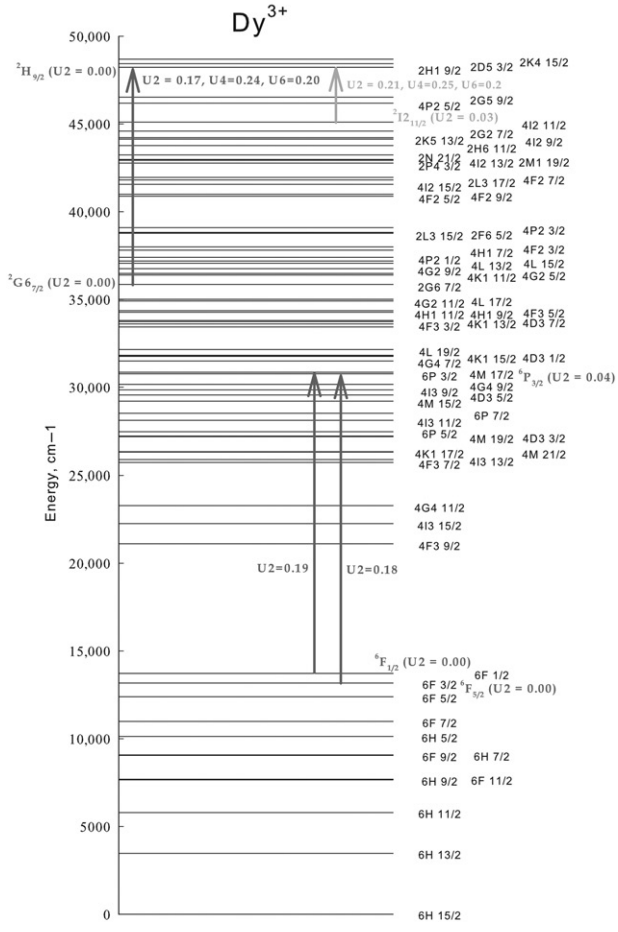

Figure 7. Perspective optical transitions in Dy^{3+}.

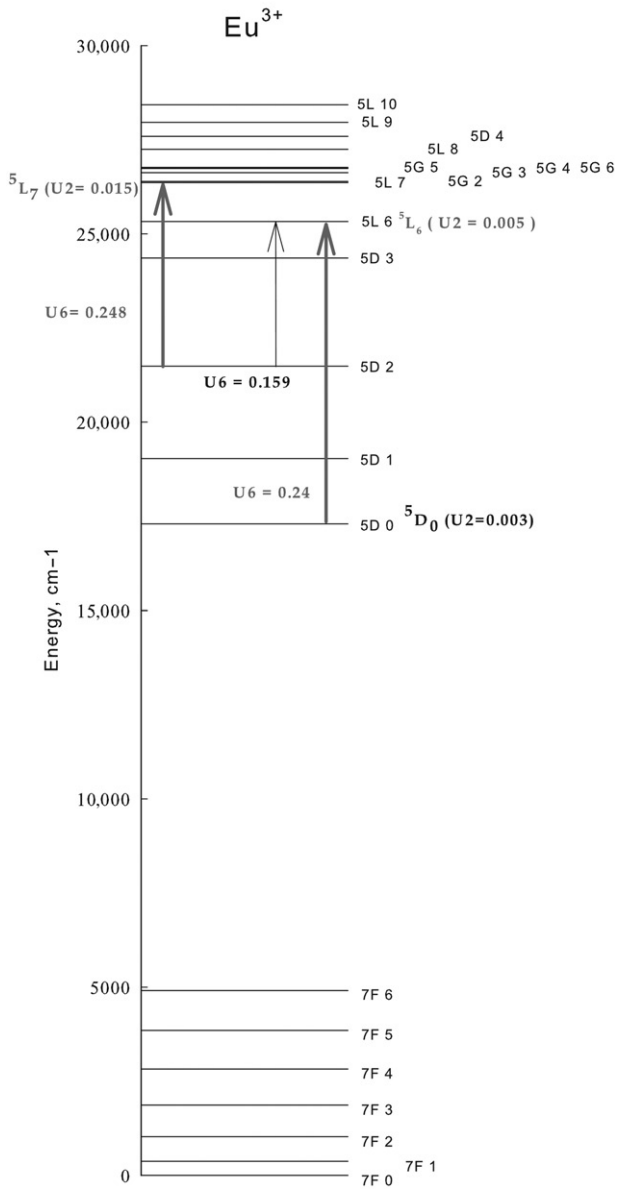

Figure 8. Perspective optical transitions in Eu^{3+}.

$^4I_{9/2} \rightarrow {}^4F_{3/2}$ in Nd, $^4I_{15/2} \rightarrow {}^4I_{13/2}$ in Er ('telecom' transition) and $^3H_6 \rightarrow {}^3H_4$ in Tm ions (our list is not exhaustive; see [2,3] for original references), the ground level is characterized by rather large U2 matrix element and thus is prone to rapid decoherence. This statement does not contradict the fact that very narrow kilohertz-range homogeneous linewidths were reported for aforementioned transitions in Pr [41,42] and Er [43,44] ions in some crystals. (Here we do not discuss the europium ion transition because this one can not be described by our approach, as has been indicated in the previous section. Nevertheless, it is worth underlining that this *0-0* transition, forbidden within the standard Judd–Ofelt theory, is much weaker than a typical transition allowed in this approximation, so in any case it would be disregarded by us as not 'strong enough'.) All these measurements were performed at extremely low temperatures, of the order of 2 K or less, and sometimes also with the use of a special configuration magnetic field [42] to decrease the influence of inter-ion interactions; in this sense such results can not be used to confirm or infer the conclusions of the present paper.

The insufficiency of the experimental decoherence data pertinent for the rare-earth ion transitions in crystals and taken in an interesting for us temperature range, around 6–50 K, makes direct comparison of our results with experiment not an easy task. However, we believe that the following example is rather instructive. For Pr^{3+} ions in $LiYF_4$ crystals, the experimentally measured values of the coefficient $\bar{\alpha}$ expressing the efficiency of the electron–phonon coupling in the context of the Raman process (of course, this process is different from direct electron–phonon transitions analyzed here, but they are nevertheless connected with each other) is more than five times smaller for the 'pre-selected' transition $^3F_2 \rightarrow {}^3P_0$ than it takes place for the non-selected and used in QIP transition from the ground level, $^3H_4 \rightarrow {}^1D_2$: they are equal, respectively, to 30 and 161 cm^{-1} [16,17]. (Moreover, this same

Table 4. Parameters of perspective optical transitions in Er^{3+}.

Ion	Initial level	Gap to the next lower level (cm^{-1})	U2 of intralevel transitions	Final level	Gap to the next lower level (cm^{-1})	U2 of intralevel transitions	Energy of the transition (cm^{-1})	Transition matrix elements U2, U4, U6
Er^{3+}	$^4G_{9/2}$	978	0.001	$^4D_{5/2}$	2001	0.001	11,095	U2 = 0.203 U6 = 0.032
	$^4F_{5/2}$	1652	0.015				16,499	U2 = 0.175
	$^4S_{3/2}$	3217	0.037				20,111	U2 = 0.212 U4 = 0.012
	$^4I_{9/2}$	2161	0.002	$^2H2_{11/2}$	796	0.002	6877	U2 = 0.208 U6 = 0.286

Table 5. Parameters of perspective optical transitions in Dy^{3+}.

Ion	Initial level	Gap to the next lower level (cm^{-1})	U2 of intralevel transitions	Final level	Gap to the next lower level (cm^{-1})	U2 of intralevel transitions	Energy of the transition (cm^{-1})	Transition matrix elements U2, U4, U6
Dy^{3+}	$^2G6_{7/2}$	846	0.00	$^2H1_{9/2}$	1707	0.00	12,376	U2 = 0.17 U4 = 0.24 U6 = 0.20
	$^4I2_{11/2}$	509	0.03				3127	U2 = 0.21 U4 = 0.25 U6 = 0.2
	$^6F_{1/2}$	548	0.00	$^6P_{3/2}$	602	0.04	17,043	U2 = 0.19
	$^6F_{5/2}$	1407	0.00				18,370	U2 = 0.18

Table 6. Parameters of perspective optical transitions in Eu^{3+}.

Ion	Initial level	Gap to the next lower level (cm^{-1})	U2 of intralevel transitions	Final level	Gap to the next lower level (cm^{-1})	U2 of intralevel transitions	Energy of the transition (cm^{-1})	Transition matrix elements U2, U4, U6
Eu^{3+}	$^5D_2$	2456	0.001	$^5L_7$	1032	0.015	4874	U6 = 0.248
	$^5D_2$	2456	0.001	$^5L_6$	970	0.005	3842	U6 = 0.159
	$^5D_0$	12,386	0.003				8032	U6 = 0.24

coefficient for the transition $^3F_2 \rightarrow {}^3P_0$ is actually the *smallest* among the six transitions of praseodymium ion investigated in [16,17] while that for the non-selected QIP transition is the largest amongst them.) This seems quite natural from the viewpoint adopted in the present paper: the total of U2, U4 and U6 values of $^3H_4$–$^1D_2$ transition (0.0717) is about 10 and 5 times smaller than U2 values within levels $^3H_4$ and $^1D_2$ correspondingly while the situation for $^3F_2 \rightarrow {}^3P_0$ is much more favorable (see Table 2). Of course, the use of transitions not involving the ground state, many of which are pre-selected here, requires step-wise laser excitation schemes, but laser step-wise excitation of rare-earth ions in crystals is nowadays well established and quite often used for realization of electromagnetic-induced transparency, study of the high-lying energy levels and so on [14]. In many cases this may present less experimental constraint than the necessity to reach very low temperatures to get rid of the electron–phonon interactions.

We would like to finish by repeating what has been already said above: we believe that the results presented on pre-selection of rare-earth ion optical transitions most suitable for QIP experiments will be useful for the specialists in the field, but detailed theoretical and, of course, first of all also experimental study of all the corresponding transitions still needs to be undertaken prior to their practical use.

Acknowledgements

One of us (S.K.S.) acknowledges the financial support of the Swiss National Science Foundation, Grant No. 200021-137711 and a Joint Science and Technology Cooperation Program Switzerland-Russia grant.

References

[1] Zoller, P.; Beth, T.; Binosi, D.; Blatt, R.; Briegel, H.; Bruss, D.; Calarco, T.; Cirac, J.I.; Deutsch, D.; Eisert, J.; Ekert, A.; Fabre, C.; Gisin, N.; Grangiere, P.; Grassl, M.; Haroche, S.; Imamoglu, A.; Karlson, A.; Kempe, J.; Kouwenhoven, L.; Kröll, S.; Leuchs, G.; Lewenstein, M.; Loss, D.; Lütkenhaus, N.; Massar, S.; Mooij, J.E.; Plenio, M.B.; Polzik, E.; Popescu, S.; Rempe, G.; Sergienko, A.; Suter, D.; Twamley, J.; Wendin, G.; Werner, R.; Winter, A.; Wrachtrup, J.; Zeilinger, A. *Eur. J. Phys. D* **2005,** *36,* 203–228.

[2] Tittel, W.; Afzelius, M.; Chanelière, T.; Cone, R.L.; Kröl, S.; Moiseev, S.A.; Sellars, M. *Laser Photonics Rev.* **2010,** *4,* 244–267.

[3] Hammerer, K.; Soerensen, A.S.; Polzik, E.S. *Rev. Mod. Phys.* **2010,** *82,* 1041–1093.
[4] Ichimura, K. *Opt. Commun.* **2001,** *196,* 119–125.
[5] Ohlsson, N.; Krishna Monah, R.; Kroell, S. *Opt. Commun.* **2002,** *201,* 71–77.
[6] Sekatskii, S.K.; Chergui, M.; Dietler, G. *Europhys. Lett.* **2003,** *63,* 21–27.
[7] Stoneham, A.M.; Fischer, A.J.; Greenland, P.T. *J. Phys.: Condens. Matter* **2003,** *15,* L447–L451.
[8] Nilsson, M.; Kroell, S. *Opt. Commun.* **2005,** *247,* 393–403.
[9] Alexander, A.L.; Longdell, J.J.; Sellars, M.J.; Manson, N.B. *Phys. Rev. Lett.* **2006,** *96,* 043602.
[10] Kraus, B.; Tittel, W.; Nilsson, M.; Kroell, S.; Gisin, M.; Cirac, J.I. *Phys. Rev. A* **2006,** *73,* 020302.
[11] Macfarlane, R.M. *J. Lumin.* **2002,** *100,* 1–20.
[12] Macfarlane, R.M. *J. Lumin.* **2007,** *125,* 156–174.
[13] Sun, Y.; Thiel, C.W.; Cone, R.L.; Equall, R.W.; Hutcheson, R.L. *J. Lumin.* **2002,** *98,* 281–287.
[14] Liu, G., Jacquier, B., Eds. *Spectroscopic Properties of Rare Earths in Optical Materials*; Springer: Berlin, 2005.
[15] Di Bartolo, B. *Optical Interactions in Solids*; World Scientific: Singapore, 2010.
[16] Ellens, A.; Andres, H.; Meijerink, A.; Blasse, G. *Phys. Rev. B* **1997,** *55,* 173–179.
[17] Ellens, A.; Andres, H.; ter Heerdt, M.L.H.; Wegh, R.T.; Meijerink, A.; Blasse, G. *Phys. Rev. B* **1997,** *55,* 180–186.
[18] Orlovskii, Y.V.; Reeves, R.J.; Powell, R.C.; Basiev, T.T.; Pukhov, K.K. *Phys. Rev. B* **1994,** *49,* 3821–3830.
[19] McCumber, D.E.; Sturge, M.D. *J. Appl. Phys.* **1963,** *34,* 1682–1684.
[20] Yen, W.M.; Scott, W.C.; Shawlow, A.L. *Phys. Rev.* **1964,** *136,* A271–A283.
[21] Henderson, B.; Imbusch, G.F. *Optical Spectroscopy of Inorganic Solids*; Clarendon Press: Oxford, 1989.
[22] Blasse, G. *Int. Rev. Phys. Chem.* **1992,** *11,* 71–100.
[23] Beck, W.; Ricard, D.; Flytzanis, C. *Phys. Rev. B* **1998,** *57,* 7694–7700.
[24] Malkin, B.Z. In *Spectroscopic Properties of Rare Earths in Optical Materials*; Liu, G., Jacquier, B., Eds.; Springer: Berlin, 2005; Chapter 3, pp 130–165.
[25] Wangsness, R.K.; Bloch, F. *Phys. Rev.* **1953,** *89,* 728–739.
[26] Bloch, F. *Phys. Rev.* **1956,** *102,* 104–135.
[27] Bloembergen, N. *Nonlinear Optics*; W.A. Benjamin: New York, 1965.
[28] Judd, B.R. *Operator Techniques in Atomic Spectroscopy*; McGraw-Hill: New York, 1963.
[29] Judd, B.R. *Phys. Rev.* **1962,** *127,* 750–761.
[30] Ofelt, G.S. *J. Chem. Phys.* **1962,** *37,* 511–520.
[31] Carnall, W.T.; Crosswhite, H.; Crosswhite, M. *Energy Level Structure and Transition Probabilities of the Trivalent Lanthanides in LaF_3*; Internal Report of Argonne National Laboratory: Argonne, IL, 1997.
[32] Kaminskii, A.A.; Mironov, V.S.; Kornienko, A.A.; Bagaev, S.N.; Boulon, G.; Brenier, A.; Di Bartolo, B. *Phys. Stat. Solidi A* **1995,** *151,* 231–255.
[33] Kaminskii, A.A.; Boulon, G.; Buoncristiani, M.; Di Bartolo, B.; Kornienko, A.A.; Mironov, V.S. *Phys. Stat. Solidi A* **1995,** *141,* 471–494.
[34] Carnall, W.T.; Fields, P.R.; Rajnak, K. *J. Chem. Phys.* **1968,** *49,* 4424–4442.
[35] Carnall, W.T.; Fields, P.R.; Rajnak, K. *J. Chem. Phys.* **1968,** *49,* 4450–4455.
[36] Tanaka, M.; Nishimura, G.; Kushida, T. *Phys. Rev. B* **1994,** *49,* 16917–16925.
[37] Smentek, L.; Wybourne, B.G. *J. Phys. B: At., Mol. Opt. Phys.* **2001,** *34,* 625–630.
[38] Kushida, T.; Tanaka, M. *Phys. Rev. B* **2002,** *65,* 195118.
[39] Sekatskii, S.K.; Basiev, T.T.; Basieva, I.T.; Dietler, G.; Fedorov, V.V.; Karasik, A.Ya.; Orlovskii, Yu.V.; Pukhov, K.K. *Opt. Commun.* **2006,** *259,* 298–303.
[40] Basiev, T.T.; Karasik, A.Ya.; Fedorov, V.V.; Ver Steeg, K.W. *J. Exp. Theor. Phys.* **1998,** *86,* 156–163.
[41] Equall, R.W.; Cone, R.L.; Macfarlane, R.M. *Phys. Rev. B* **1995,** *52,* 3963–3969.
[42] Fraval, E.; Sellars, M.J.; Longdell, J.J. *Phys. Rev. Lett.* **2004,** *92,* 077601.
[43] Böttger, T.; Thiel, C.W.; Sun, Y.; Cone, R.L. *Phys. Rev. B* **2006,** *74,* 075107.
[44] Böttger, T.; Thiel, C.W.; Cone, R.L.; Sun, Y. *Phys. Rev. B* **2008,** *77,* 155125.